Non-linear 3D Visual Control for an Unmanned Aerial Vehicle

Daniel D. Guevara and Víctor H. Andaluz

Universidad de las Fuerzas Armadas ESPE, Sangolquí, Ecuador
{ddguevara1, vhandaluz1}@espe.edu.ec

Abstract. This document presents the development of a kinematic control with visual feedback based on images, to solve the objective tracking problem in the semi-structured 3D workspace in UAV. The design of the entire controller is based on a total Jacobian that contains the geometric, image, and object Jacobian. These Jacobians allow the calculation of the control errors that feedback the system through the characteristics of the image, allowing the stability and robustness of the system to be determined. The system implementation was developed by calibrating the UAV's vision sensor against a global reference system, using the Python programming language, which is the means of communication between the PC and the UAV, in the same way with MATLAB mathematical software.

Keywords: UAV Visual Control, Stability Analysis and Robustness.

1 Introduction

Unmanned Aerial Vehicles (UAVs) play important roles in both, the consumer and commercial markets. Compared to manned aircrafts, UAVs are generally much more cost effective, smaller, able to approach dangerous areas and there-fore widely applied in search and rescue, emergency, delivery, infrastructure inspection and others [1, 2, 3]. A basic requirement for a UAV is autonomous and robust navigation and positioning, which will be carried out using vision-based control techniques. Computer vision is gaining importance in the field of mobile robots, currently used in the feedback control cycle, as a cheap, passive and in-formation-rich tool. The vision sensor, usually combined with an inertial measurement unit (IMU) provides solid information about an object, allowing autonomous positioning and navigation [4,5].

When designing a Computer Vision system, a number of parameters are always taken into account that will be decisive for the appearance of the objects in the image to be the best for the subsequent analysis algorithms. However, for those Computer Vision algorithms that need to extract three-dimensional information from an image or image sequence or to establish the correspondence between two or more cameras, the calibration of the intrinsic and extrinsic parameters of the vision system is a fundamental step [6]. In this study, a camera with a large field of view is adopted to simplify the development and validation of the servo-visual control approach [7]. Currently there is

a lot of work related to visual servo control [8] based on path-following images [6] for manipulators [1], mobile robots and drones [9, 10,11].

In the present research work it is proposed to implement a control with visual feedback in closed loop for the recognition and monitoring of 3D patterns by means of an unmanned aerial vehicle (UAV), based on the characteristics of movement of the aerial robot and the projection of the characteristic points of the image of the pattern to be followed. In addition, the stability and robustness of the proposed control scheme is mathematically analyzed in order to ensure that control errors tend to zero. Finally, the performance of the proposed controller in partially structured work environments was evaluated experimentally. It is important to emphasize that this research focuses on several important points such as pattern detection [6], mathematical modelling and control scheme presented in the section 2 y 3. Inside the controller. It is worth mentioning that the models found will be used to determine the Jacobian matrix of the system, that is, the relationship between the Jacobian Image (vision sensor) and the Jacobian Geometry (UAV) presented in section 2.

2 System Structure

The servo visual handheld camera control technique increases effective resolution and prevents obstruction of the target by the application in mobile robots such as UAVs. The system is composed of a visual sensor integrated into the UAV, so the geometric modelling of the robot is proposed as an integrated structure. The kinematic model of a UAV results in the location of the point of interest as a function of the location of the UAV. The kinematic model of a UAV gives the derivative of its location of the point of interest according to the location of the aerial mobile platform, $\dot{\mathbf{h}} = \partial f / \partial \boldsymbol{\theta}(\theta)\mathbf{v}$, where $\dot{\mathbf{h}} = \left[\dot{h}x\ \dot{h}y\ \dot{h}z\ \dot{\theta}\right]^T$ is the velocity vector at the point of interest, is the mobility control vector of the mobile air handler, in this case the dimension depends on the manoeuvring velocities of the UAV.

It is indispensable to enunciate the kinematic model of the UAV from the linear and angular velocity, in this way its movement can be initiated, in such a way the following kinematic model is obtained [1]

$$\dot{\mathbf{h}}(t) = \mathbf{J}_{\mathbf{g}}(\theta)\mathbf{v}(t) \tag{1}$$

where, $\dot{\mathbf{h}} \in \mathbb{R}^n$ with $n = 4$ represents the vector of the velocities of the axis of the system $\sum_o$ and the angular velocity around the Z axis; the Jacobian matrix that defines a linear mapping between the vector of velocities $\mathbf{v}(t)$ of the UAV; and the maneuverability control of the UAV is defined as $\mathbf{v} \in \mathbb{R}^m$ with $m = 4$ represents the velocity vector of the UAV $\mathbf{v} = \left[\ v_l \quad v_m \quad v_n \quad \omega\right]$, from the reference system $\sum_c$.

2.1 Mathematical Model of the Visual Sensor

The camera model used in this document is the perspective projection model or pinhole model. This implies a simplified model for an ideal viewing camera without distortion and without optical noise. The projection perspective with the Pinhole camera model is shown in Markus Richter [1], where f_c is the focal length, ${}^{w}\mathbf{p}_i \in \Re^3$ y ${}^{c}\mathbf{p}_i = \begin{bmatrix} {}^{c}x_i & {}^{c}y_i & {}^{c}z_i \end{bmatrix}^T \in \Re^3$ are the 3D position vectors of the *ith* characteristic point of the target object in relation to $\sum_o$ y $\sum_c$, respectively, as shown in Fig. 1.

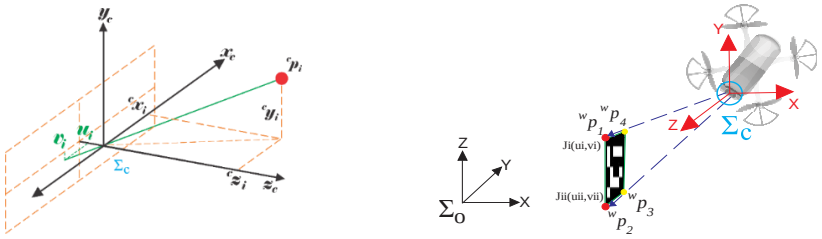

(a) Projection perspective of the UAV with the pattern to follow.

(b) Frame of reference for a UAV with visual feedback through selected points.

Fig. 1. Projection perspective of the characteristic image points.

3 Controller design and stability analysis

A. Design Controller

This Section discusses the design of a visual controller based on image feature errors (image-based control) to enable a UAV with a built-in camera to perform a task of tracking moving objects in the 3D workspace, while image feature errors are defined as $\xi(t)$ converge asymptotically to zero. Therefore, the control objective can be defined as $\lim_{t\to\infty} \tilde{\xi}(t) = 0$. Depending on the frame of reference $\sum_o$ represents the framework of the world and $\sum_c$ is the frame of the camera, as shown in Fig. using a transformation of coordinates, plus the relationship between them is expressed this way, ${}^{c}\mathbf{p}_i = {}^{c}\mathbf{R}_w \left({}^{w}\mathbf{p}_i - {}^{c}\mathbf{p}_{Corg} \right)$. The perspective projection of the *ith* characteristic point in the plane of the image gives us the coordinate of the plane of the image $\xi_i = \begin{bmatrix} u_i & v_i \end{bmatrix}^T \in \Re^2$ as

$$\xi_i \left({}^{c}x_i, {}^{c}y_i, {}^{c}z_i \right) = -\frac{f_c}{{}^{c}z_i} \begin{bmatrix} {}^{c}x_i \\ {}^{c}y_i \end{bmatrix} \tag{2}$$

solving (2) and ${}^{c}\mathbf{p}_i$, it can be expressed as follows $\dot{\xi}_i$ in terms of UAV velocity as

$$\dot{\xi}_i = \mathbf{J}_{\mathbf{I}_i}\left(\xi_i, {}^c z_i\right)\begin{bmatrix} {}^c\mathbf{R}_w & 0 \\ 0 & {}^c\mathbf{R}_w \end{bmatrix}\mathbf{J}_{\mathbf{g}}\left(\boldsymbol{\theta}\right)\mathbf{v} - \mathbf{J}_{\mathbf{o}_i}\left(\boldsymbol{\theta}, {}^c\mathbf{p}_i\right){}^w\dot{\mathbf{p}}_i \tag{3}$$

where $\mathbf{J}_{\mathbf{g}}\left(\boldsymbol{\theta}\right)$ is the *Jacobian geometric* UAV defined in Eq. (1), $\mathbf{J}_i\left(\xi_{i,}\, {}^c z_i\right)$ is the *jacobian of image* defined by $\mathbf{J}_{\mathbf{I}_i}\left(\xi_i, {}^c z_i\right)$. In addition, $\mathbf{J}_{\mathbf{o}_i}\left(\boldsymbol{\theta}, {}^c\mathbf{p}_i\right){}^w\dot{\mathbf{p}}_i$ represents the movement of the *ith* characteristic point in the plane of the image, where ${}^w\dot{\mathbf{p}}_i$ is the velocity of the *ith* point in relation to $\sum_o$ and $\mathbf{J}_{\mathbf{o}_i}\left(\boldsymbol{\theta}, {}^c\mathbf{p}_i\right)$. [1]

In applications where the object is in a 3D workspace, two or more image characteristics are needed for the visual servo control to be implemented [8, **12,** 13]. To extend this model to r image points it is necessary to stack the vectors of the coordinate of the image plane, that is, $\xi = \begin{bmatrix} \xi_1^T & \xi_2^T & \xi_3^T & \ldots & \xi_r^T \end{bmatrix}^T \in \Re^{2r}$ and ${}^c\mathbf{p} = [\,{}^c\mathbf{p}_1 \quad {}^c\mathbf{p}_2 \quad \ldots \quad {}^c\mathbf{p}_r\,]^T \in \Re^{3r}$. It is assumed that multiple point entities are provided in a known object. From Eq. (3), for multiple point entities one can written

$$\dot{\xi} = \mathbf{J}\left(\boldsymbol{\theta}, \xi, {}^c z\right)\mathbf{v} - \mathbf{J}_{\mathbf{o}}\left(\boldsymbol{\theta}, {}^c\mathbf{p}\right){}^w\dot{\mathbf{p}} \tag{4}$$

where

$$\mathbf{J}\left(\boldsymbol{\theta}, \xi, {}^c z\right) = \mathbf{J}_{\mathbf{I}}\left(\xi, {}^c z\right)\begin{bmatrix} {}^c\mathbf{R}_w & 0 \\ 0 & {}^c\mathbf{R}_w \end{bmatrix}\mathbf{J}_{\mathbf{g}}(\boldsymbol{\theta}); \qquad \mathbf{J}_{\mathbf{I}}\left(\xi, {}^c z\right) = \begin{bmatrix} \mathbf{J}_{\mathbf{1}}\left(\begin{bmatrix} u_1 & v_1 \end{bmatrix}^T, {}^c z_1\right) \\ \vdots \\ \mathbf{J}_r\left(\begin{bmatrix} u_r & v_r \end{bmatrix}^T, {}^c z_r\right) \end{bmatrix};$$

$$\mathbf{J}_{\mathbf{o}}\left(\boldsymbol{\theta}, {}^c\mathbf{p}\right) = \begin{bmatrix} \dfrac{f_c}{{}^c z_1}\begin{bmatrix} 1 & 0 & -\dfrac{{}^c x_1}{{}^c z_1} \\ 0 & 1 & -\dfrac{{}^c y_1}{{}^c z_1} \end{bmatrix} & \ldots & \dfrac{f_c}{{}^c z_m}\begin{bmatrix} 1 & 0 & -\dfrac{{}^c x_r}{{}^c z_r} \\ 0 & 1 & -\dfrac{{}^c y_r}{{}^c z_r} \end{bmatrix} \end{bmatrix}^T {}^c\mathbf{R}_w$$

For the sake of simplicity, the following notation will now be used $\mathbf{J} = \mathbf{J}\left(\boldsymbol{\theta}, \xi, {}^c z\right)$ and $\mathbf{J}_{\mathbf{o}} = \mathbf{J}_{\mathbf{o}}\left(\boldsymbol{\theta}, {}^c\mathbf{p}\right)$. This section, an image is captured at the desired reference position and the corresponding extracted characteristics represent the desired characteristics vector ξ_d. The control problem is to design a controller that calculates the velocities applied $\mathbf{v}_{\mathbf{ref}}$ to move the UAV in such a way that the characteristics of the actual image reach the desired ones. The design of the kinematic controller is based on the kinematic model of the UAV and the projection model of the camera. Eq. (4), $\mathbf{v}$ can be expressed in terms of $\dot{\xi}$ and ${}^w\dot{\mathbf{p}}$ using the pseudo-inverse matrix $\mathbf{J}$, *i.e.*, $\mathbf{v} = \mathbf{J}^{\#}\left(\dot{\xi} + \mathbf{J}_{\mathbf{o}}{}^w\dot{\mathbf{p}}\right)$ where, $\mathbf{J}^{\#} = \mathbf{W}^{-1}\mathbf{J}^{\mathbf{T}}\left(\mathbf{J}\mathbf{W}^{-1}\mathbf{J}^{\mathbf{T}}\right)^{-1}$, being $\mathbf{W}$ a positive defined matrix that weighs on the control actions of the system, $\mathbf{v} = \mathbf{W}^{-1}\mathbf{J}^T\left(\mathbf{J}\mathbf{W}^{-1}\mathbf{J}^T\right)^{-1}\left(\dot{\xi} + \mathbf{J}_{\mathbf{o}}{}^w\dot{\mathbf{p}}\right)$. The controller is based on a

simple solution, where you will reach your navigation target with as few movements as possible. The following control law is proposed for the visual control of the UAV,

$$\mathbf{v}_{ref} = \mathbf{J}^{\#}\left(\mathbf{J}_{\mathbf{o}}\,{}^{w}\dot{\mathbf{p}} + \mathbf{L}_{\mathbf{K}}\tanh\left(\mathbf{L}_{\mathbf{K}}^{-1}\mathbf{K}\tilde{\xi}\right)\right) \tag{5}$$

where, $\mathbf{J}_{\mathbf{o}}\,{}^{w}\dot{\mathbf{p}}$ represents the velocity of the object to follow in the plane of the image, $\tilde{\xi}$ is the vector of control errors defined as $\tilde{\xi} = \xi_d - \xi$, $\mathbf{K} \in \Re^{2r}$, $\mathbf{L}_{\mathbf{K}} \in \Re^{2r}$.

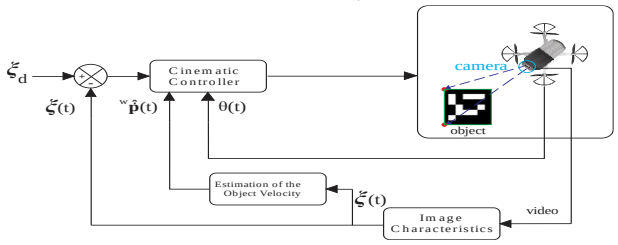

Fig. 2. Scheme of control of the complete system.

The mission of the UAV is based on the values of the image characteristics corresponding to the relative positions of the robot and the object in the image plane. In this approach, an image is captured at the desired reference position and the corresponding extracted characteristics represent the desired characteristic vector ξ_d. The problem with visual control is to design a controller that calculates the applied $\mathbf{v}_{ref}$ velocities to move the UAV in such a way that the real image characteristics reach the desired ones. To solve the problem of visual control a complete control scheme of the system is proposed as shown in Fig. 2. The error in the image is defined as $\tilde{\xi} = \xi_d - \xi$, it can be calculated at any time during the measurement and used to operate the mobile manipulator in a direction that reduces the error. Therefore, the purpose of the control is to ensure that $\lim_{t\to\infty}\tilde{\xi}(t) = 0 \in \Re^{2r}$.

How, the behavior of the control error $\tilde{\xi}$ is analyzed assuming a perfect follow up of the velocity $\mathbf{v} = \mathbf{v}_{ref}$, $\mathbf{v}_{ref} = \begin{bmatrix} v_l & v_m & v_n & \omega \end{bmatrix}^T$. It must be taken into account that the vector of the desired image characteristic is constant, therefore, it can be concluded that $\dot{\tilde{\xi}} = -\dot{\xi}$. Now, substituting Eq. (5) in Eq. (4) gives the following closed-loop equation is obtained, $\tilde{\xi} + \mathbf{L}_{\mathbf{K}}\tanh\left(\mathbf{L}_{\mathbf{K}}^{-1}\mathbf{K}\tilde{\xi}\right) = 0$. For the stability analysis the following Lyapunov candidate function is considered $V\left(\tilde{\xi}\right) = \frac{1}{2}\tilde{\xi}^{\mathbf{T}}\tilde{\xi}$. Its time derivative on the trajectories of the system is, $\dot{V}\left(\tilde{\xi}\right) = -\tilde{\xi}^{\mathbf{T}}\mathbf{L}_{\mathbf{K}}\tanh\left(\mathbf{L}_{\mathbf{K}}^{-1}\mathbf{K}\tilde{\xi}\right) < 0$ which implies that $\tilde{\xi}(t) \to \mathbf{0}$ asymptotically.

4 Robustness Analysis

In some studies of visual servo controller based on image do not choose to perform an analysis of stability and robustness [14,15], in this document does not exclude all this analysis because it is a fundamental part of the controller to determine that it is valid, consistent and especially applicable experimentally in any mobile device, as in our case in a UAV [16].

The proposed controller presented above considers that the velocity of the object to follow ${}^{w}\dot{\mathbf{p}}$ is exactly known. However, this is not always possible in a real context. In practice, this velocity will be estimated using visual detection of the position of the object, *e.g.* by means of a filter $\alpha-\beta$ [17]. This motivates to study the behavior of the image characteristic error $\tilde{\xi}$ considering the estimated velocity errors of the object to follow and also considering the assumption of a perfect velocity tracking. It defines the velocity estimation errors of the object in the image plane as $\varepsilon = \mathbf{Jo}\left({}^{w}\hat{\dot{\mathbf{p}}} - {}^{w}\dot{\mathbf{p}}\right)$ where ${}^{w}\hat{\dot{\mathbf{p}}}$ y $\hat{\dot{\mathbf{p}}}$ are the actual and estimated velocities of the object, respectively. Hence $\tilde{\xi} + \mathbf{L_K}\tanh\left(\mathbf{L_K^{-1}K}\tilde{\xi}\right) = 0$ can now written as

$$\tilde{\xi} + \mathbf{L_K}\tanh\left(\mathbf{L_K^{-1}K}\tilde{\xi}\right) = \mathbf{J}\tilde{\mathbf{v}} + \varepsilon \tag{6}$$

Lyapunov candidate function $V\left(\tilde{\xi}\right) = \frac{1}{2}\tilde{\xi}^{\mathbf{T}}\tilde{\xi}$ is considered again, which time derivative along the trajectories of the system Eq. (6) is $\dot{V}\left(\tilde{\xi}\right) = \tilde{\xi}^{\mathbf{T}}\left(\mathbf{J}\tilde{\mathbf{v}} + \varepsilon\right) - \mathbf{L_K}\tanh\left(\mathbf{L_K^{-1}K}\tilde{\xi}\right)$. A sufficient condition for $\dot{V}\left(\tilde{\xi}\right)$ to be negative definite is

$$\left|\tilde{\xi}^{\mathbf{T}}\mathbf{L_K}\tanh\left(\mathbf{L_K^{-1}K}\tilde{\xi}\right)\right| > \left|\tilde{\xi}^{\mathbf{T}}\left(\mathbf{J}\tilde{\mathbf{v}} + \varepsilon\right)\right| \tag{7}$$

For large values of $\tilde{\xi}$, it can be considered that $\mathbf{L_K}\tanh\left(\mathbf{L_K^{-1}K}\tilde{\xi}\right) \approx \mathbf{L_K}$. Then, Eq.(7) can be expressed as $\|\mathbf{L_K}\| > \|\mathbf{J}\tilde{\mathbf{v}} + \varepsilon\|$ thus, making the errors $\tilde{\xi}$ decrease. Now, for small values of $\tilde{\xi}$, $\mathbf{L_K}\tanh\left(\mathbf{L_K^{-1}K}\tilde{\xi}\right) \approx \mathbf{K}\tilde{\xi}$, thus Eq. (7) can be written as, $\|\tilde{\xi}\| > \|\mathbf{J}\tilde{\mathbf{v}} + \varepsilon\| / \lambda_{\min}(\mathbf{K})$ thus, implying that the error $\tilde{\xi}$ is bounded by, $\|\tilde{\xi}\| \le \|\mathbf{J}\tilde{\mathbf{v}} + \varepsilon\| / \lambda_{\min}(\mathbf{K})$. Hence, it is concluded that the image feature error is ultimately bounded by the bound $\|\mathbf{J}\tilde{\mathbf{v}} + \varepsilon\| / \lambda_{\min}(\mathbf{K})$ on a norm of the control error and the estimated velocity error the object to be followed.

5 Experimental Results

Both tests were carried out to evaluate the performance of the proposed controller, the first in real time using Python software as a means of communication between the PC

with the Tello UAV of the DJI brand and the second test by simulation in the MATLAB mathematical software.

Experiment 1: The experimental tests are in a semi-structured environment or with little influence from wind, where the linear velocities have a very low margin of error, in the same way the angular velocity is stable most of the time. These control actions are observed in Fig. 3. y Fig. shows that the control errors $\tilde{\xi}(t)$ are ultimately bounded with final values close to zero, i.e., achieving final feature errors max $\left(\left|\tilde{\xi}(t)\right|\right)$ < 40 pixels with a sampling of 250 milliseconds.

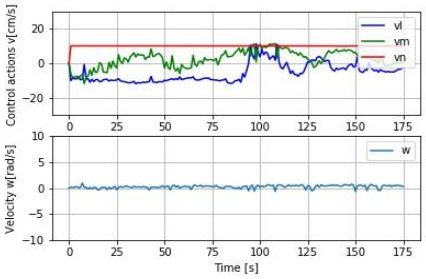

Fig. 3. Actions to control the linear velocities received by the UAV.

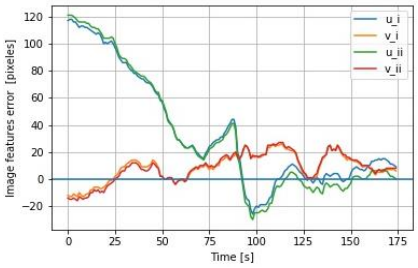

Fig. 4. Time evolution of control error $\tilde{\xi}(t)$.

Experiment 2: This experiment is a simulation result performed to evaluate the performance of the system when the target makes a movement in 3D space. In Fig. it is observed that the control actions tend to zero in a very short period of time, as in Fig. the control errors are minimal with a sampling of 100 milliseconds, demonstrating the theory of control. Fig. shows the strobe movement of the UAV with respect to the characteristic image points in the workspace (X, Y and Z).

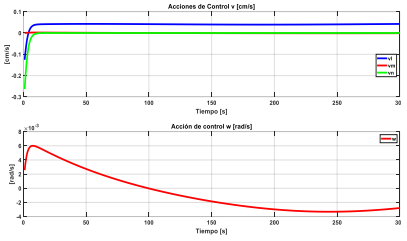

Fig. 5. Velocities commands to the UAV.

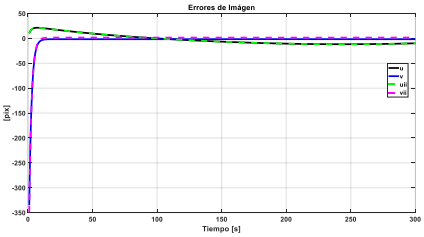

Fig. 6. Time evolution of control error $\tilde{\xi}(t)$.

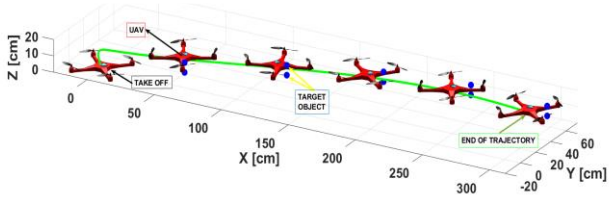

Fig. 7. Strobe movement of the UAV. UAV position and target position are displayed at the same instant. Five different moments of time are represented.

Acknowledgment. The authors would like to thank the Coorporación Ecuatoriana para el Desarrollo de la Investigación y Academia CEDIA for their contribution in innovation, through the CEPRA projects, especially the project CEPRA-XIII-2019-08; Sistema Colaborativo de Robots Aéreos para Manipular Cargas con Óptimo Consumo de Recursos; also Universidad de las Fuerzas Armadas ESPE and the Research Group ARSI, for the support for the development of this work.

References

1. R. C. L. S. J. M. T. F. R. Víctor Andaluz, «Visual control with adaptive dynamical compensation for 3D target tracking,» *Mechatronics*, vol. 22, nº 4, p. 491, 24 Octubre 2011.
2. N. I. Siegwart R, «Introduction to autonomous mobile robots,» *The MIT*, 2004.
3. W. L. B. S. J. W. C. Y. &. C. C. K. Zhou, "Position control of a tail-sitter UAV using successive linearization based model predictive control.," *Control Engineering Practice 91*, p. 104125, 2019.
4. S. M. J. F. &. S. G. S. Saripalli, «Vision-based autonomous landing of an unmanned aerial vehicle,» de *Cat. No. 02CH37292*, Washington, DC, USA, USA, 11-15 May 2002.
5. S. R. H. L. R. &. C. P. Salazar, «Modeling and real-time stabilization of an aircraft having eight rotors,» *In Unmanned Aircraft Systems*, pp. 455-470, 2008.
6. J. A. J. P. J. G. Arturo dela Escalera, «Detección Automática de un Patrón para la Calibración de Cámaras,» *Revista Iberoamericana de Automática e Informática Industrial RIAI*, vol. 7, nº 4, pp. 83-94, 2010.
7. Z. H. Z. Gangqi Dong, «Kinematics-based incremental visual servo for robotic capture of non-cooperative target,» *Robotics and Autonomous Systems*, vol. 112, pp. 221-228, 2019.
8. R. F. Andaluz Victor, «Robust control with redundancy resolution and dynamic compensation for mobile manipulators.,» *IEEE-ICIT international conference on induatrial technology*, pp. 1449-1454, 2010.
9. R. M. Tarek Hamel, «Image based visual servo control for a class of aerial robotic systems,» *Automatica*, vol. 43, nº 11, pp. 1975-1983, 2007.
10. C. T. M. R. Z. K. E. D. J. C. S.S. Mehta, «New approach to visual servo control using terminal,» *Journal of the Franklin Institute*, vol. 356, pp. 5001-5026, 2019.
11. P. I. Corke, «Visual control of robot manipulators–a review.,» *World Scientific Series in Robotics and Intelligent SystemsVisual Servoing*, pp. 1-31, 1993.
12. R. P. E. B. Chaumette F, «Classification and realization of the different vision-based tasks.,» *In Visual Servoing: Real-Time Control of Robot Manipulators Based on Visual Sensory Feedback* , pp. 199-228, 1993.
13. K. A. A. &. N. T. Hashimoto, «Visual servoing with redundant features.,» *Journal of the Robotics Society of Japan*, vol. 16, nº 3, pp. 384-390, 1998.
14. E. A. Zehra Ceren, «Image Based and Hybrid Visual Servo Control,» *Journal of Intelligent & Robotic Systems*, vol. 65, nº 1-4, pp. pp 325-344, January 2012.
15. T. Yüksel, «An intelligent visual servo control,» *Transactions of the Institute of Measurement and Control*, vol. 41, pp. pp 3-13, 2019.
16. F. R. J. M. T. J. M. S. a. R. C. Jorge A. Sarapura, «Visual Servo Controllers for an UAV,» *Machine Vision and Navigation*, pp. pp 597-625, January 2020.
17. P. R. Kalata, «The Tracking Index: A Generalized Parameter for α-β and α-β-γ Target Trackers,» *IEEE Transactions on Aerospace and Electronic Systems*, Vols. %1 de %2AES-20, nº 2, pp. 174 - 182, 1984.